Proceedings of the 5th International Conference on Fluid Flow and Thermal Science (ICFFTS 2024)
Lisbon, Portugal- November 21 - 23, 2024
Paper No. 108
DOI: 10.11159/icffts24.108

Numerical Prediction of the Aerodynamic Forces by Applying a New Turbulence Model

Yaser H Alahmadi[1]
[1]Islamic University of Madinah
Abo Bakr Al Siddiq, Al Jamiah, Madinah 4235, Saudi Arabia
yhalahmadi@iu.edu.sa

Abstract **-** Numerous turbulence models have emerged in recent decades for the purpose of simulating aerodynamic flows. The utilization of eddy viscosity models (EVM) to address Reynolds Averaged Navier-Stokes (RANS) equations yields results of considerable accuracy for flow fields. Furthermore, EVMs are favoured due to their resilience and computational efficiency. Nevertheless, achieving both precision and effectiveness in the development of a turbulence model remains a significant challenge. The current study delves into the analysis of the external flow around the NACA0012 airfoil. It assesses the effectiveness of the recently introduced Shear Stress Transport Model with Curvature Correction Modification (SSTCCM) in forecasting the flow characteristics of external aerodynamic flows. Previous research has demonstrated the SSTCCM model's adeptness in accurately predicting intricate internal flows, such as cyclone separators [YH Alahmadi et al., 2016. Chem. Eng. Sci. 147(6),150-165], rotating lids, and sudden expansion [YH Alahmadi et al., 2021. Ind. Eng. Chem. Res. 6016–6026]. Nevertheless, the SSTCCM model has not yet been scrutinized for scenarios involving external flows where the aerodynamic configuration significantly impacts flow behaviour. Consequently, this present study represents the inaugural exploration of the efficacy of the SSTCCM turbulence model in forecasting aerodynamic flow attributes. The outcomes of the computational simulations are juxtaposed with experimental data gathered by NASA for validation, and also verified against alternative RANS models. The SSTCCM model showcases its proficiency in accurately estimating aerodynamic coefficients. Additionally, the findings indicate that the SSTCCM model outperforms traditional Eddy Viscosity Models (EVMs) in the prediction of lift and drag coefficients, particularly at the angle of attack corresponding to stall.

Keywords**:** CFD, Fluid Dynamics, Aerodynamics, SSTCCM, External Flow, NACA 0012, Turbulence Models.

1. Introduction

Computational Fluid Dynamics (CFD) is an essential tool for analysing and predicting various fluid flow problems. Recently, the need for numerical simulations has grown rapidly across multiple industries where fluid flow plays a crucial role. CFD analyses are generally categorized into three types: Direct Numerical Simulation (DNS), Large Eddy Simulation (LES), and Reynolds-Averaged Navier-Stokes (RANS). Due to the high computational resources required for DNS and LES, their application is limited, this allows the RANS simulations to be more practical for most engineering purposes [3, 5].

One particularly challenging area in CFD is the numerical analysis of aerodynamic forces, as the complex flow patterns around such geometries make it difficult to achieve accurate results. Selecting an appropriate turbulence model for these kinds of flows is a complicated task. Among many models, the newly developed Shear Stress Transport with Curvature Correction Modification (SSTCCM) shows promise. This model has recently demonstrated its ability to predict flow characteristics in complex flow phenomena.

The SSTCCM model was initially introduced by Alahmadi and Nowakowski in 2016 [2], where they modified the k-ω SST model by adding a rotation function to address the limitations of traditional Eddy Viscosity Models (EVMs). Their research focused on simulating highly swirling flows in a gas-cyclone separator and showed a strong correlation between the numerical predictions and experimental results, proving the SSTCCM's superiority over standard EVMs. In 2021, Alahmadi et al. expanded on this by simulating swirling flow with vortex breakdown to compare SSTCCM results with other turbulence models [1]. They validated the model against laboratory measurements for flows within a closed cylinder with a rotating lid and through a sudden expansion pipe. The results confirmed the model's precision and reliability, making it highly useful for various engineering applications. However, the model had not been tested in external flow cases where aerodynamic shapes strongly affect flow behavior.

This study aims to evaluate the recently developed SSTCCM model's ability to predict and simulate external flows. The NACA 0012 airfoil was chosen as the case study due to the abundance of experimental and numerical data available for comparison.

A significant limitation of EVMs is their inability to accurately capture the effects of rotating systems. When dealing with swirling flows, EVMs fail to properly represent the "free-loss vortex" part of the Rankine vortex near the wall. The use of the Boussinesq hypothesis in EVMs leads to an assumption of isotropic eddy viscosity, which is not valid for complex flows like cyclones. Several modifications have been proposed to address this issue, but many lack the general applicability required for 3D flows [6, 10, 14].

Knight and Saffman [12], and Spalart and Shur [16], suggested empirical modifications to EVMs to account for rotation and curvature effects. Knight and Saffman's approach is more efficient as it captures the impact of invariant turbulence components and provides a unified explanation for the model's handling of curvature and rotation. This makes their method easier to apply to 3D flows. Additionally, Hellsten improved the k-ω SST model by incorporating the effects of system rotation and streamlined curvature [9]. One specific modification Hellsten introduced was changing the definition of the Richardson number (Ri), replacing the turbulent time scale from the Khodak and Hirsch model [11] with the mean-flow time scale $1/S_{ij}$. These modifications improved the model's representation of flow characteristics and enhanced its predictive capabilities.

In 2009, Smirnov and Menter [15] further advanced the SST k-ω model by incorporating Spalart and Shur's rotation curvature correction function [16]. This adaptation focused on correcting the production terms in the turbulent kinetic energy and dissipation rate equations, resulting in the SSTCC model. The SSTCC model improved in accuracy, computational efficiency, and robustness, particularly for flows involving strong rotation or curvature. By including the curvature correction function, the SSTCC model provided more accurate predictions of flow behavior while also reducing computational demands.

In 2013, Zhang and Yang introduced a simpler method to account for system rotation and curvature in the Spalart-Allmaras model. Their approach used the Richardson number (Ri) to avoid the complex calculation of Lagrangian derivatives of the strain rate tensor, streamlining the process [17].

The NACA 0012 airfoil is commonly used as a benchmark for studying aerodynamic properties. For example, Guo et al [8], investigated the flow field and aerodynamic characteristics of the NACA 0012 airfoil in a biplane MVA configuration. This study aims to assess how well the SSTCCM model captures turbulence characteristics and flow behavior around the NACA 0012 airfoil.

2. Governing Equations and Turbulence Modelling:

2.1. Navier-Stokes Equations

The fluid flow around the NACA 0012 airfoil can be described using the Navier-Stokes equations, which express the conservation of momentum and continuity. These can be written in the following form using Einstein notation:

1. Continuity equation:

$$\frac{\partial u_i}{\partial x_i} = 0 \qquad (1)$$

This equation ensures that mass is conserved in the flow.

2. Momentum equation:

$$\rho \frac{\partial u_i}{\partial t} + \rho \frac{\partial u_i u_j}{\partial x_j} = -\frac{\partial p}{\partial x_i} + \frac{\partial}{\partial x_j}\left(2\mu s_{ij}\right) \quad (2)$$

where u represents the velocity vector, p is the pressure, and the strain-rate tensor (s_{ij}) is given by:

$$s_{ij} = \frac{1}{2}\left(\frac{\partial u_i}{\partial x_j} + \frac{\partial u_j}{\partial x_i}\right) \quad (3)$$

These equations, when time-averaged, result in the Reynolds-Averaged Navier-Stokes (RANS) equations. In this approach, the flow quantities, such as velocity and pressure, are decomposed into time-averaged components and fluctuations. The RANS equations are expressed as:

3. Time-averaged continuity equation:

$$\frac{\partial \overline{u_i}}{\partial x_i} = 0 \quad (4)$$

4. Time-averaged momentum equation:

$$\rho \frac{\partial \overline{u_i}}{\partial t} + \rho \frac{\partial \overline{u_i u_j}}{\partial x_j} = -\frac{\partial \bar{p}}{\partial x_i} + \frac{\partial}{\partial x_j}\left(2\mu S_{ij} - \rho \acute{u}_i \acute{u}_i\right) \quad (5)$$

Here, the additional nonlinear term $-\rho \acute{u}_i \acute{u}_i$, which appears in the RANS equations, represents the Reynolds stress tensor. To address this nonlinear term and "close" the set of equations, a turbulence model is necessary.

2.2. The SSTCCM Model

In 2016, Alahmadi and Nowakowski introduced a modified version of the Shear Stress Transport (SST k-ω) turbulence model [2], which incorporated a correction function to account for rotation and curvature effects. This model, known as SSTCCM, applies a rotation correction function to the production terms in the turbulence transport equations for k (turbulent kinetic energy) and ω (specific dissipation rate). This modification eliminates the need for Lagrangian derivatives and additional terms, simplifying the model. The modified transport equations for *k* and ω in the SSTCCM model are:

1. Transport equation for turbulent kinetic energy *k*:

$$\frac{\partial(\rho k)}{\partial t} + \frac{\partial(\rho u_j k)}{\partial x_j} = P_k f_{rot} - \beta^* \rho k \omega + \frac{\partial}{\partial x_j}\left[\mu_{ef} \frac{\partial k}{\partial x_j}\right] \quad (6)$$

2. Transport equation for specific dissipation rate ω:

$$\frac{\partial(\rho \omega)}{\partial t} + \frac{\partial(\rho u_j \omega)}{\partial x_j} = \alpha \frac{\rho P_k}{\mu_t} f_{rot} - D_\omega + C d_\omega + \frac{\partial}{\partial x_j}\left[\mu_{ef} \frac{\partial \omega}{\partial x_j}\right] \quad (7)$$

In these equations, f_{rot} represents the rotation correction function, which adjusts the turbulence equations to account for rotation and curvature effects. The function $f_{rot}$is given by:

$$f_{rot} = max\{min(f_{r1}, 1.25), 0.0\} \quad (8)$$

where f_{r1} is defined by more complex relationships between flow properties. These modifications allow the model to more accurately predict flow behavior, especially in situations where rotation and curvature play significant such as swirling flows.

3. Numerical Implementation and Simulation Setup:

3.1. Solver and Algorithm

The SSTCCM turbulence model was implemented on the open-source platform, OpenFOAM 2.4.0 [7]. This code uses a finite volume method for spatial discretization, and an unsteady solver is applied to simulate the incompressible flow field. In all simulations, the PIMPLE algorithm was employed to couple the velocity and pressure fields. This algorithm is a combination of the PISO and SIMPLE algorithms, commonly used for transient simulations involving fluid flows [4].

3.2. Mesh Generation and Simulation Settings

The accuracy of a numerical solution, along with its computational cost, heavily depends on the quality of the grid or mesh used. Mesh generation can be divided into structured, semi-structured (hybrid), and unstructured types. Errors in numerical simulation usually stem from the shape and size of the grid cells, while the computational cost is largely influenced by the resolution of the grid.

The primary metrics for assessing mesh quality include factors such as skewness, cell orthogonality, and aspect ratio. Generating a structured grid for complex geometries can be particularly challenging, as sharp edges—like the trailing edge of an airfoil—add further complexity to the mesh creation process. This complexity often requires additional mesh refinement to correct for non-orthogonal faces. To address these challenges and improve robustness, a non-orthogonal sub-algorithm corrector was applied to adjust calculations in cases of non-orthogonality.

A grid-independence study was conducted to determine the optimal grid size. The study used three different grid sizes, as shown in Table 1. The results revealed that denser grids yielded minimal improvements in calculating the lift coefficient C_L, but significantly increased the number of non-orthogonal faces, which unnecessarily escalates computational costs.

Table 1. Dimensionless lift coefficient C_L of different grid sizes.

	Grid Size	**Non-orthogonal**	**orthogonal corrector**	**C_L**
Coarse	78,256	153	1	0.812525
Medium	115,200	257	2	0.854006
Fine	400,145	894	4	0.854462

For the simulations presented in the following sections, the medium mesh size, which consists of 115,200 cells, was used. This grid configuration is shown in Figure 1.

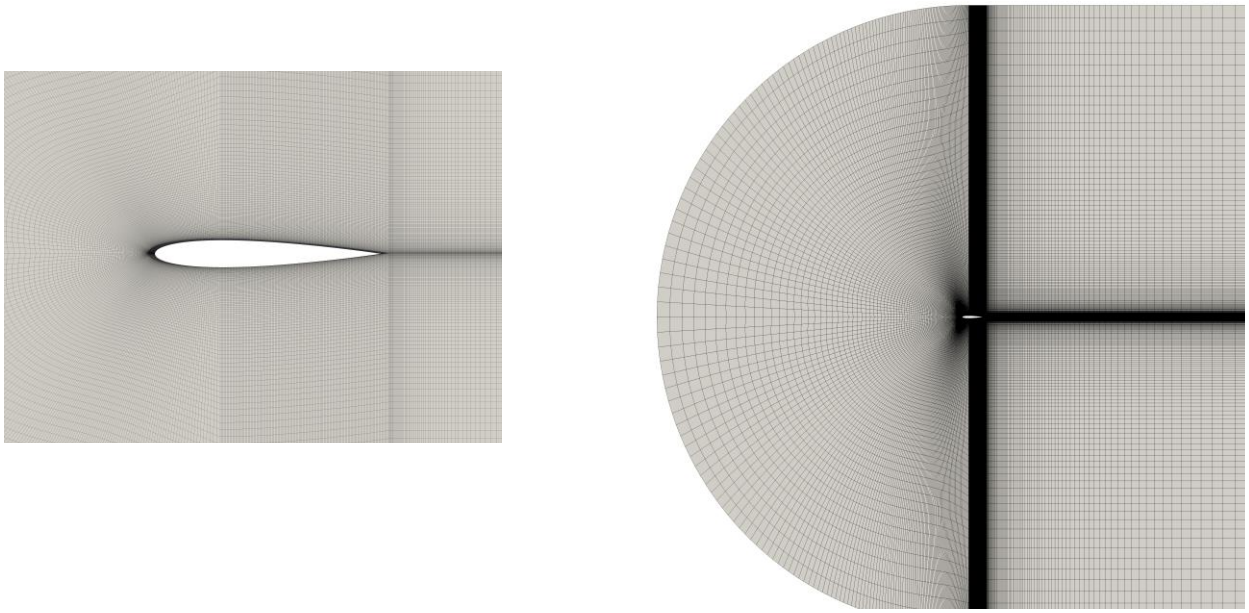

Fig. 1: Grid generation of the computational domain with medium size.

The flow domain for this study is presented in Figure 2. The chord-based Reynolds number for the simulation is Re = 3.92×10^5, and the velocity profile and corresponding inlet turbulent flow quantities were derived from preliminary calculations for fully developed turbulent flow in a two-dimensional channel. The dynamic viscosity ν, was set to 1.568×10^{-5} (m^2/s). At the inlet, a Dirichlet boundary condition was applied with $U_{in} = 51\, m/s$, while no-slip conditions were enforced on the fixed walls and zero-gradient conditions were imposed at the outlet. All the boundary conditions used in the simulations are summarized in Table 2.

Table 2: The setup of boundary conditions.

Boundary	$\boldsymbol{U}(m/s)$	$\boldsymbol{p}(\mathrm{kg}/(m \cdot s^2))$	$\mathbf{k}(m^2/s^2)$	$\boldsymbol{\omega}(1/s)$	$\boldsymbol{\nu_t}(m^2/s)$
Inlet	$(u_x, 0, 0)$	zero gradient	$2/3\,(IU)^2$	$5U/L$	$\boldsymbol{k/\omega}$
Outlet	zero gradient	0	zero gradient	zero gradient	zero gradient
Wall	$(0, 0, 0)$	zero gradient	0	$10\frac{6\nu}{\beta_1(\Delta y)^2}$	0
airfoil	$(0\ ,0, 0)$	zero gradient	0	$10\frac{6\nu}{\beta_1(\Delta y)^2}$	0

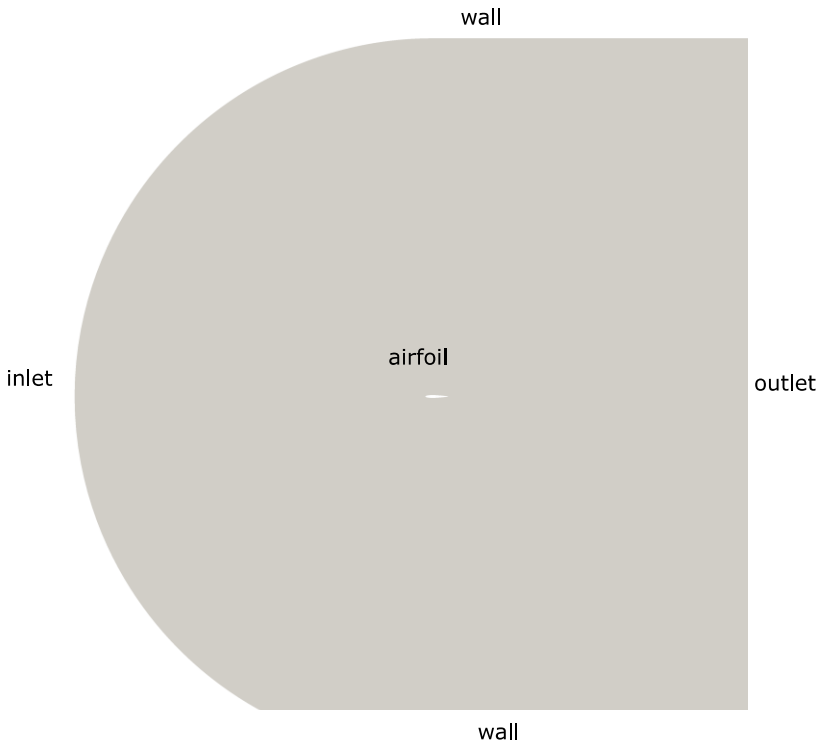

Figure 1. Computational domain and the physical boundaries.

4. Results

The To demonstrate the effectiveness of the newly developed SSTCCM model in predicting external flows, a series of simulations were carried out for the NACA 0012 airfoil at different angles of attack (α). The experimental data used for comparison in this study were taken from Ladson's research [13].

Figures 3 and 4 compare the numerical predictions with experimental measurements of the lift and drag coefficients, respectively, at varying angles of attack. The results show that the k-ϵ model does not perform well, as it overestimates the lift coefficient while underestimating the drag coefficient. Other models demonstrate higher accuracy, particularly in the linear region of the lift coefficient (CL) versus the angle of attack (AoA). However, significant differences between the numerical results and experimental data become apparent near the stall angle.

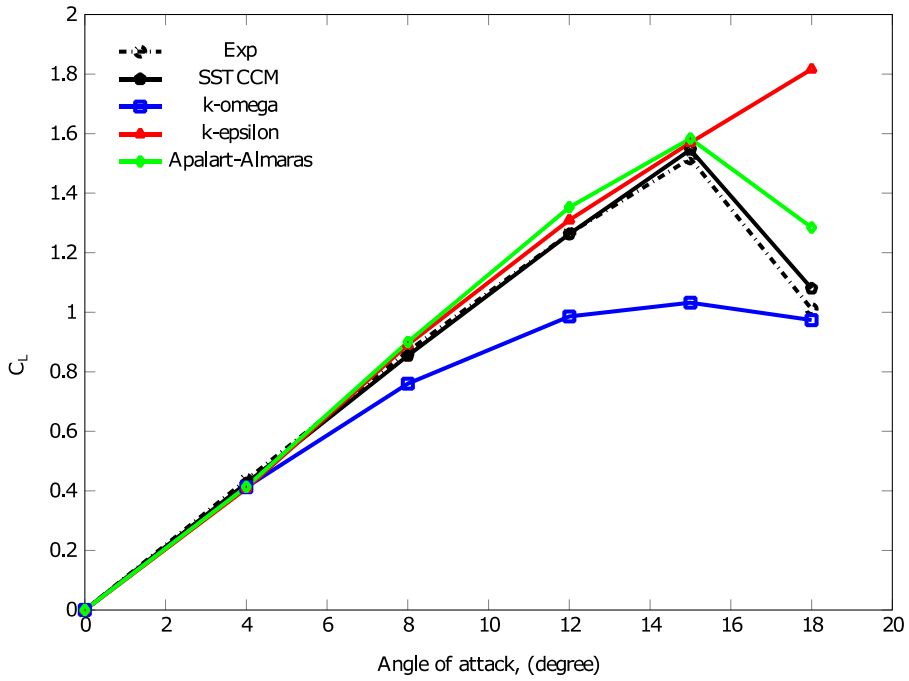

Figure 3. Lift coefficient vs angle of attack.

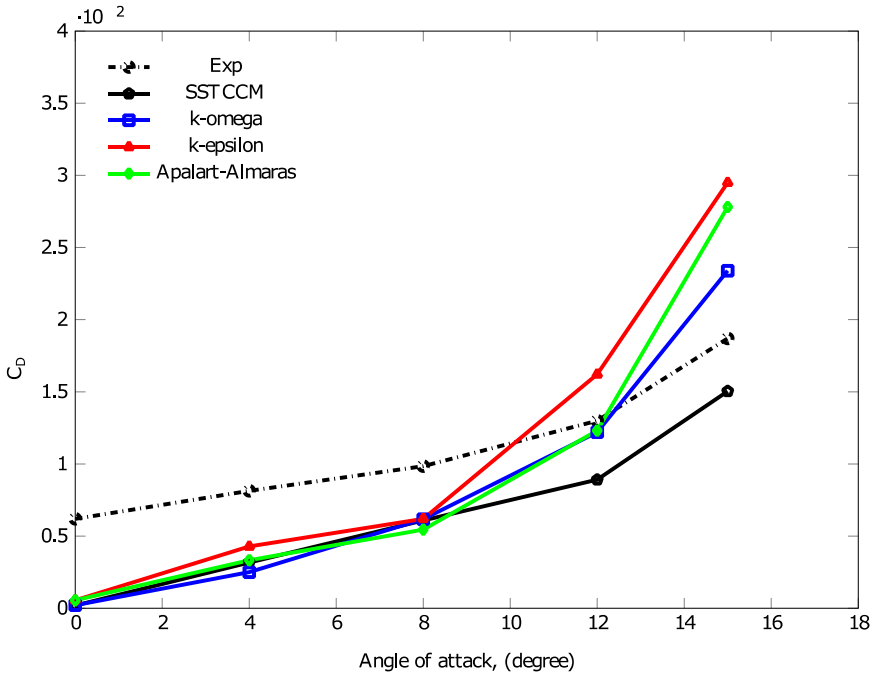

Figure 4. Drag coefficient vs angle of attack.

The SSTCCM model shows the closest agreement with experimental data, particularly for predicting the lift and drag coefficients. In contrast, the Spalart-Allmaras (S-A) model tends to slightly overpredict the maximum lift coefficient, C_{Lmax}. Additionally, while other models such as the SST k-ω model fail to accurately capture the stalling behaviour at higher angles of attack, the SSTCCM model performs better in this regard, especially in terms of lift coefficient predictions.

In the case of drag coefficient validation, the RANS simulations tend to underestimate the drag coefficient in pre-conditions. Around an angle of attack of 12°, just before the stall, the k-ϵ and S-A models predict the drag coefficient with high accuracy, whereas the SST k-ω and SSTCCM models are less accurate in this range. The significant flow separation occurring in the stall region introduces instability in the flow and the generation of vortices, making the predictions more challenging. During this phase, the flow behaviour shows a large discrepancy between computational and experimental data. The aerodynamic coefficients were calculated based on the average values from the last time step of the simulation. Figure 5 shows the averaging process for the drag coefficient at $\alpha = 4°$ using the SSTCCM model.

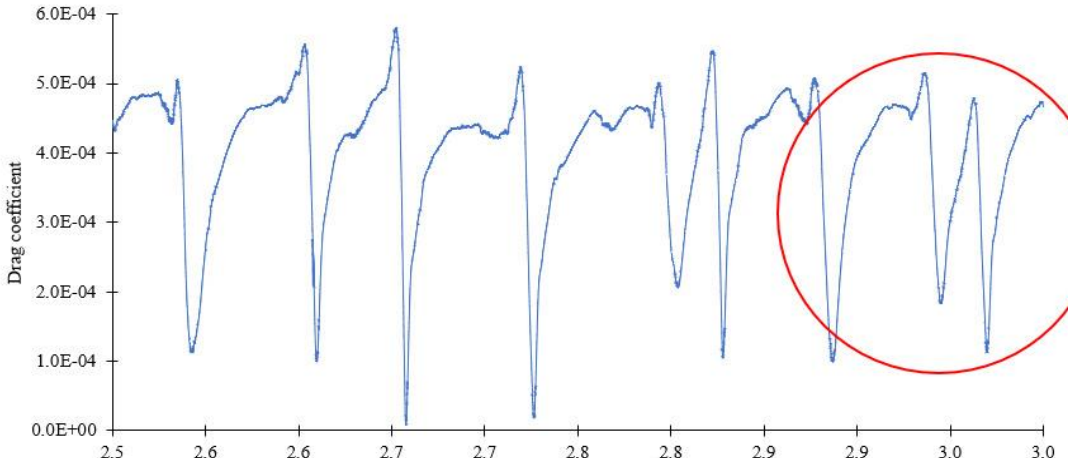

Figure 5. The calculation of drag coefficient over the simulated time.

The pressure contours at different angles of attack (α = 4°, 15°, and 18°) are shown in Figures 6, 7, and 8, respectively, for various turbulence models at a time step of 0.01 seconds. At pre-stall conditions, all turbulence models yield similar pressure distributions. The difference in pressure between the upper and lower surfaces of the airfoil generates the lift force. As the angle of attack increases to the stall region, the SSTCCM model better predicts the pressure distribution, which results in smaller errors in the aerodynamic forces. However, with the exception of the k-ϵ model, all turbulence models exhibit similar behaviour.

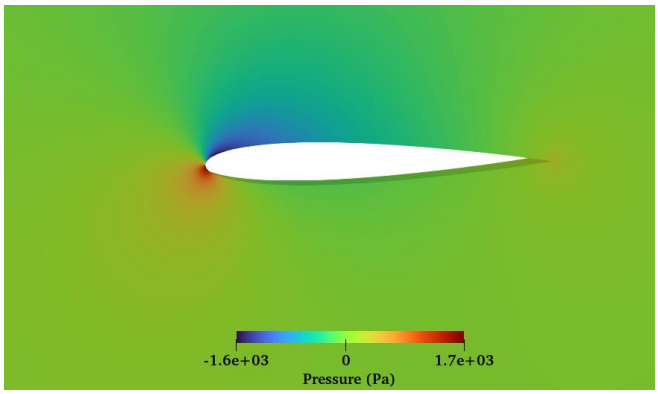

(a) k − ϵ turbulence model

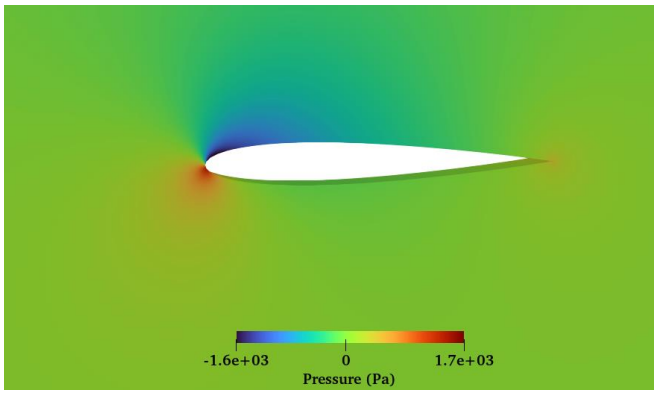

(b) S − A turbulence model

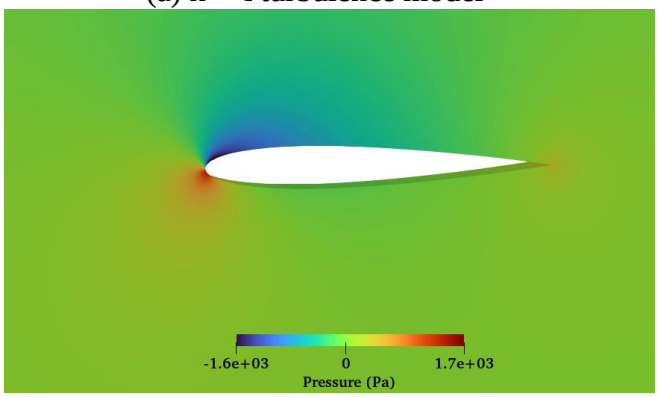

(c) k − ω turbulence model

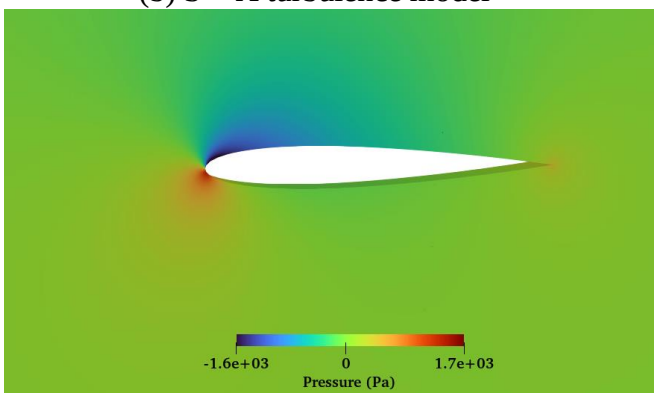

(d) SSTCCM turbulence model

Figure 6. The pressure contour of different turbulence models at α = 4° and time step 0.01 s.

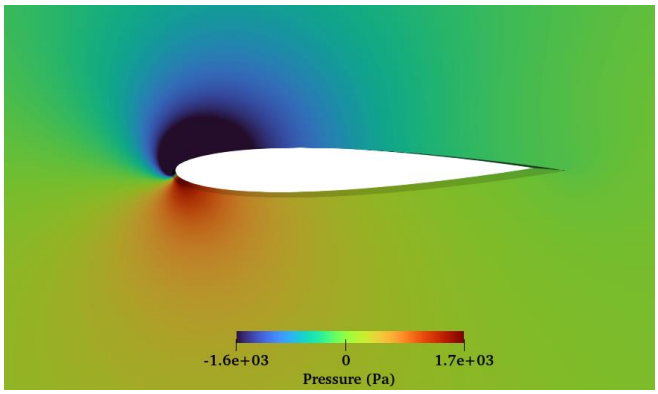

(a) k − ϵ turbulence model

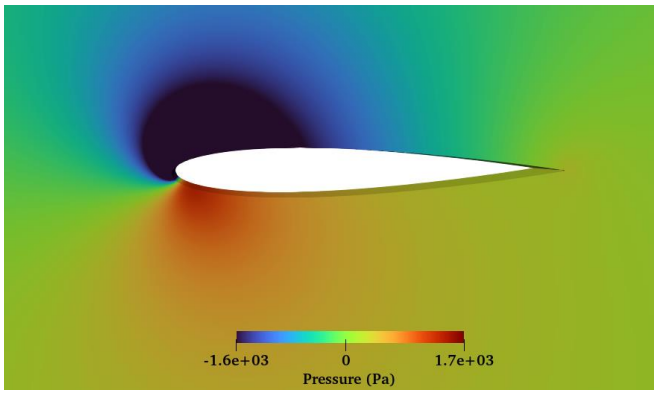

(b) S − A turbulence model

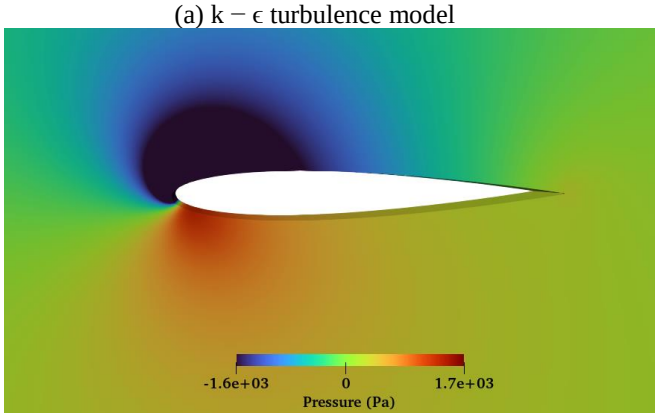

(c) k − ω turbulence model

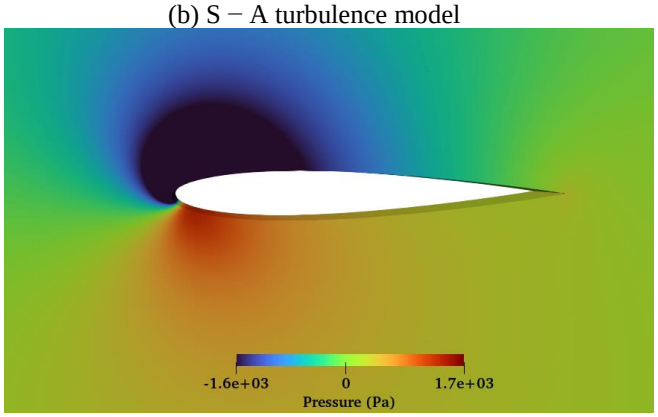

(d) SSTCCM turbulence model

Figure 7. The pressure contour of different turbulence models at α = 15° and time step 0.01 s

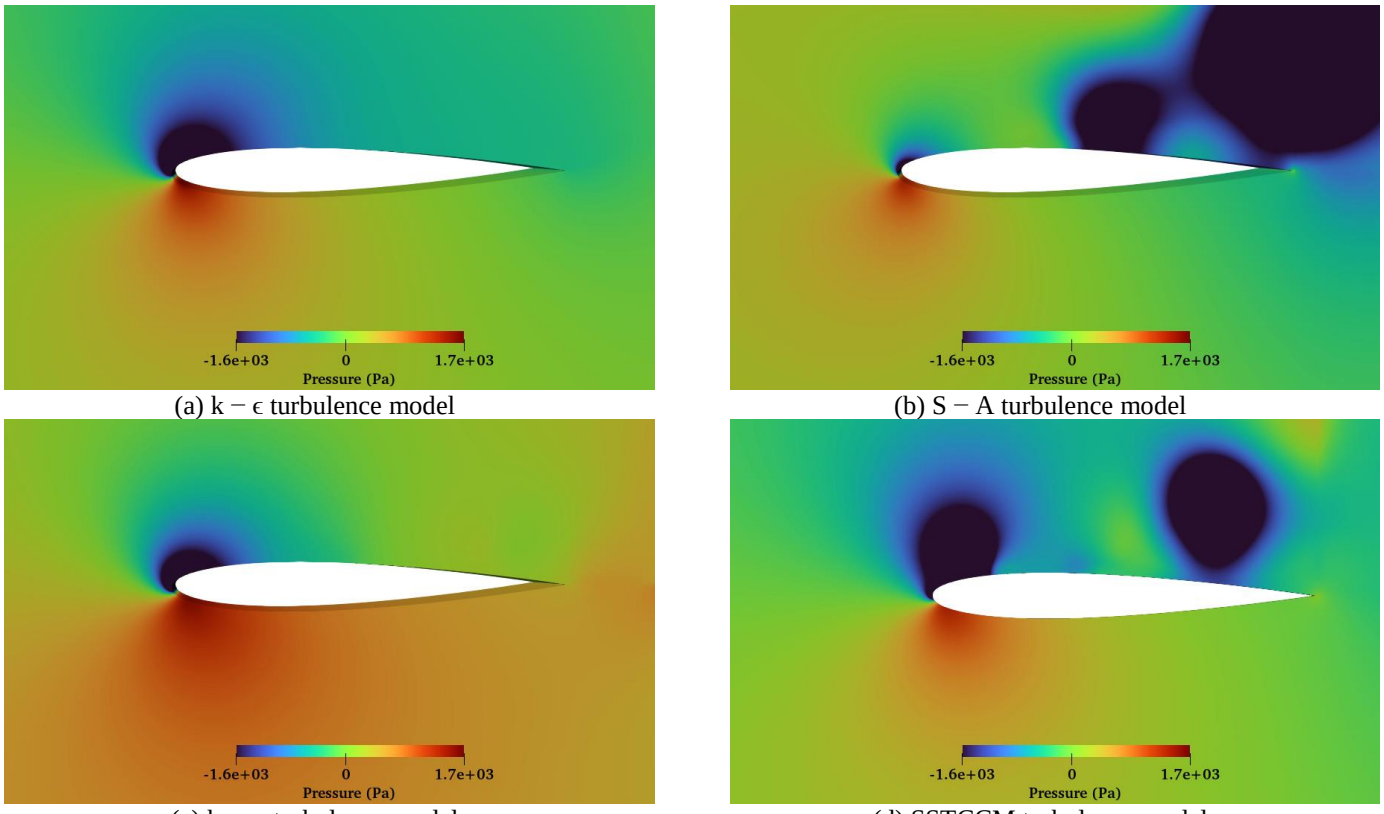

(a) k − ϵ turbulence model (b) S − A turbulence model

(c) k − ω turbulence model (d) SSTCCM turbulence model

Figure 8. The pressure contour of different turbulence models at α = 18° and time step 0.01 s

At post-stall conditions, the SSTCCM turbulence model continues to show its ability to accurately predict the pressure distribution, as seen during the stall. Figures 9, 10, and 11 illustrate the velocity contours and streamlines for pre-stall, stall, and post-stall conditions, respectively, at a time step of 0.01 seconds. At α = 4°, the flow remains attached to the airfoil surface, with no noticeable flow separation. Flow separation begins at various locations depending on the turbulence model used and becomes fully detached at post-stall angles of attack. The SSTCCM model provides the most accurate representation of flow separation compared to the other models, leading to the best agreement with experimental results. The SST k-ω and S-A models also perform reasonably well under most conditions but struggle to capture the flow behavior accurately at α = 18°.

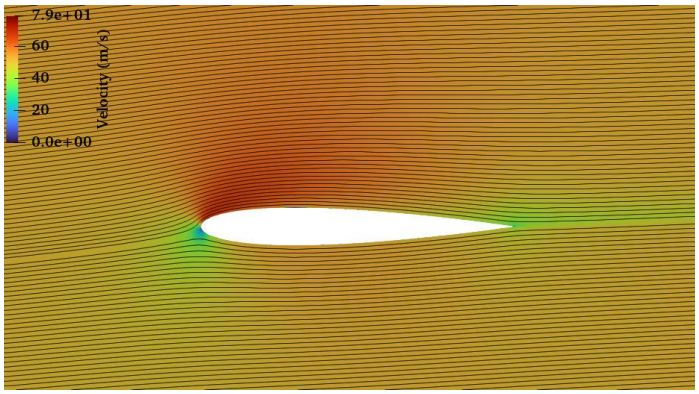

(a) k − ϵ turbulence model

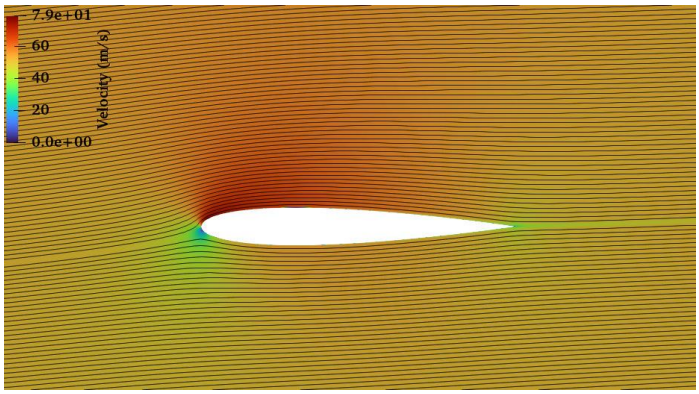

(b) S − A turbulence model

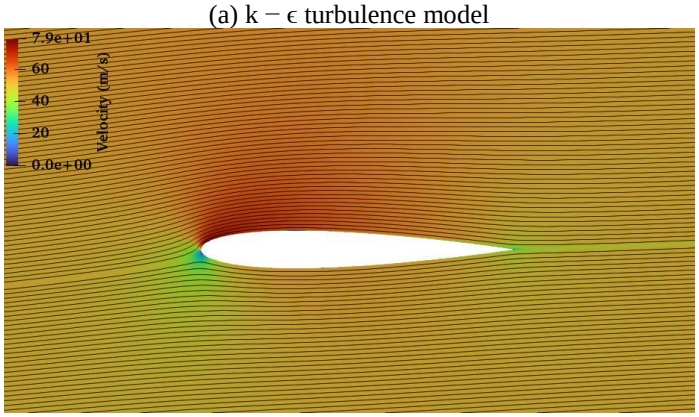

(c) k − ω turbulence model

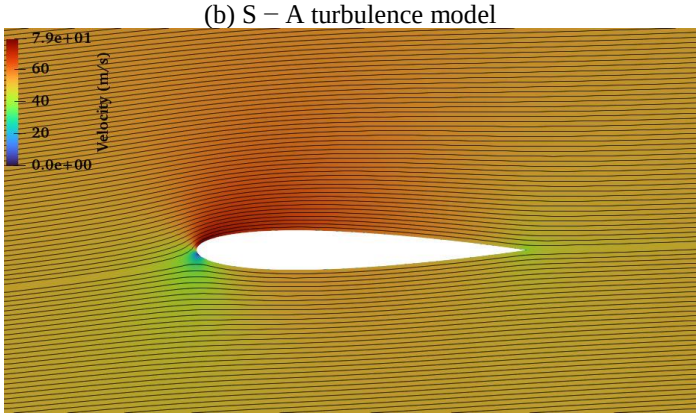

(d) SSTCCM turbulence model

Figure 9. The velocity contour and streamlines α = 4° and time step 0.01 s

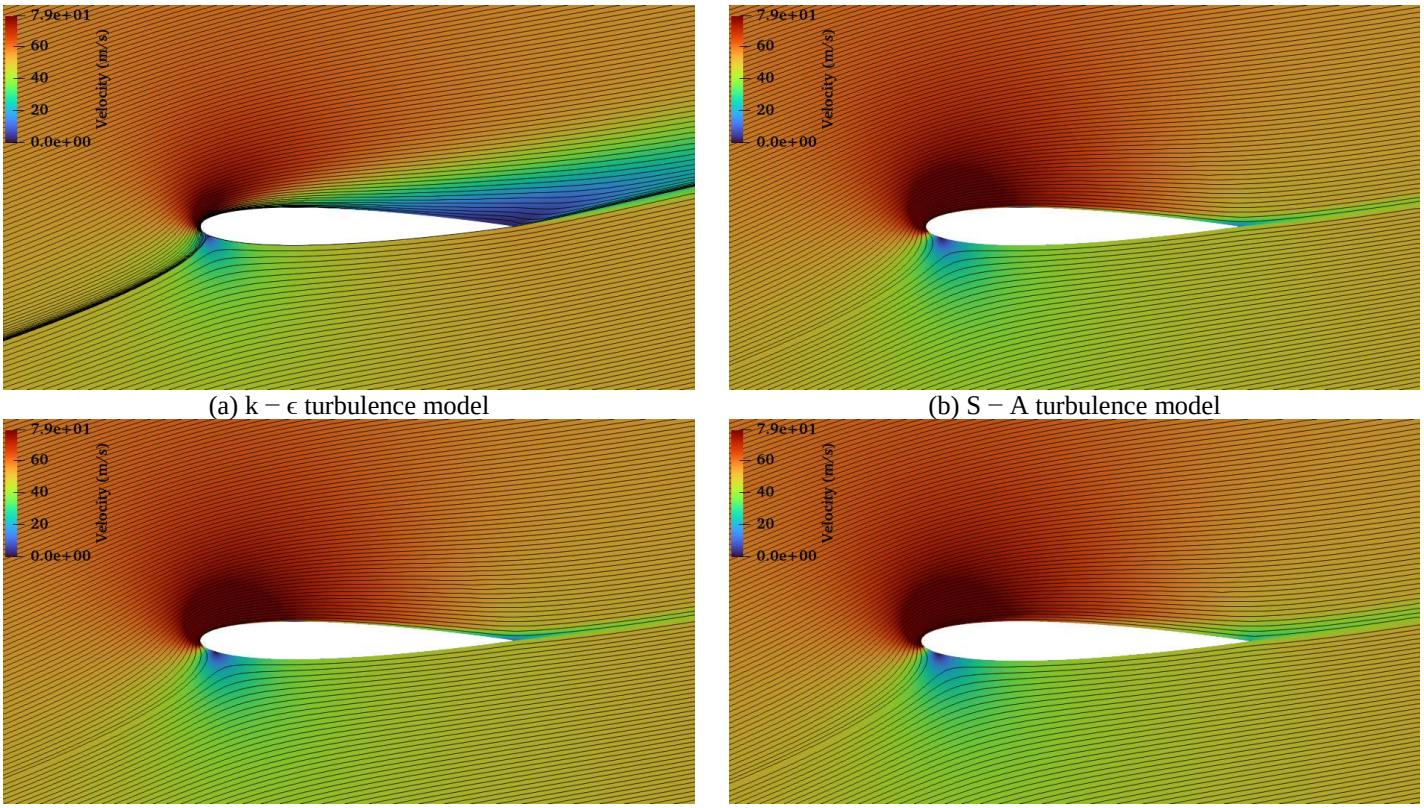

(a) k − ϵ turbulence model (b) S − A turbulence model

(c) k − ω turbulence model (d) SSTCCM turbulence model

Figure 10. The velocity contour and streamlines α = 15° and time step 0.01 s

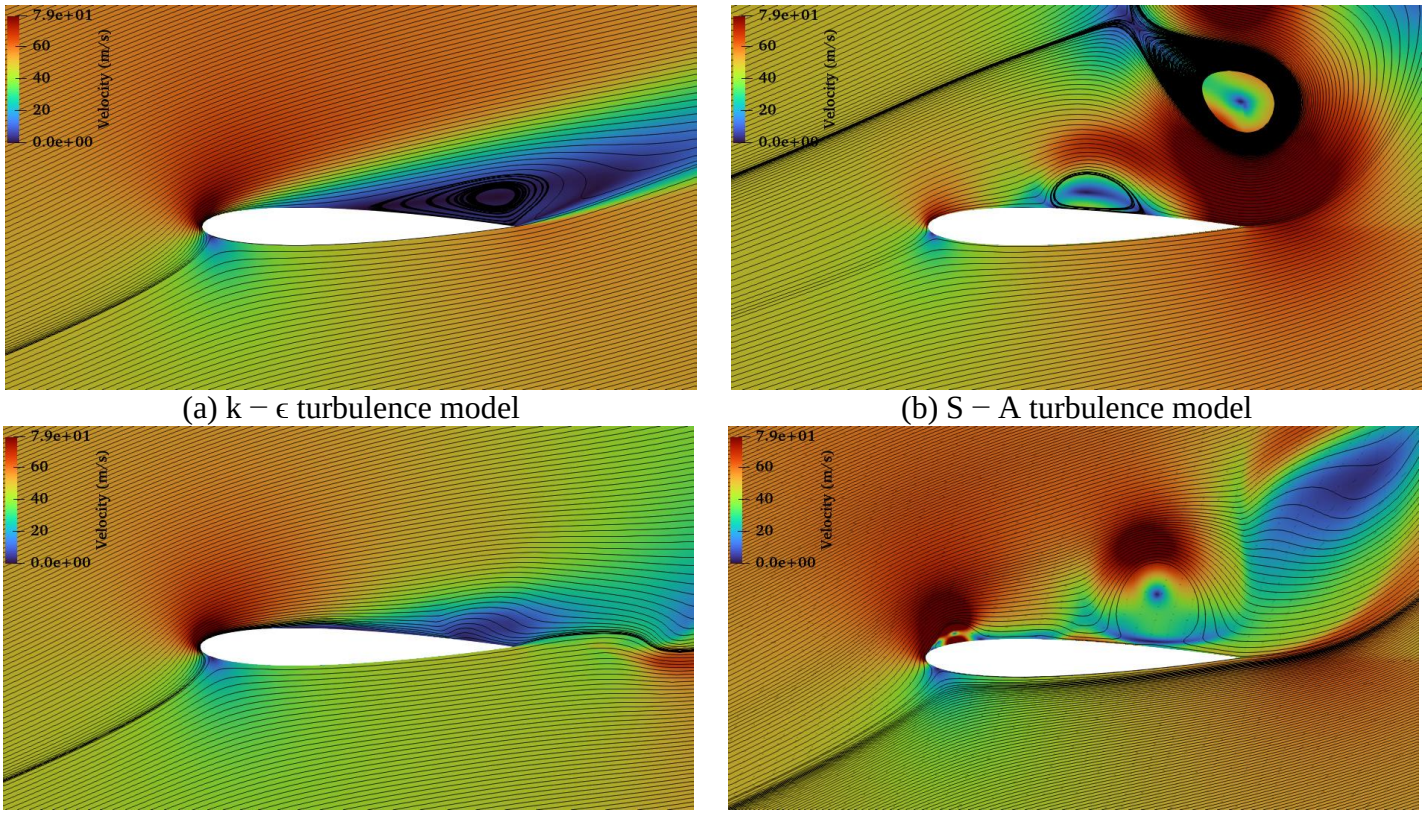

(a) k − ϵ turbulence model (b) S − A turbulence model

(c) k − ω turbulence model (d) SSTCCM turbulence model

Figure 11. The velocity contour and streamlines α = 18° and time step 0.01 s

5. Conclusion

Conclusions The newly modified SSTCCM (Shear Stress Transport with Curvature Correction Modification) eddy viscosity turbulence model was used in this study to evaluate its ability to simulate external aerodynamic flows around a NACA 0012 airfoil. This research represents the first time the model has been applied to external flow simulations. The numerical predictions from the SSTCCM model show good agreement with the experimental data obtained by Ladson [13].

The model was tested across various flow regimes and angles of attack, demonstrating its ability to accurately predict flow separation and the recirculation zone at high angles of attack. When compared to conventional Eddy Viscosity Models (EVMs), the SSTCCM model consistently outperformed them, particularly in estimating aerodynamic forces such as lift and drag across all angles of attack.

Acknowledgements

The author would like to express his appreciation for the support provided by the Scientific Research Deanship, Islamic University of Madinah.

References

[1] Y. H. Alahmadi, S. A. Awadh, and A. F. Nowakowski, "Simulation of swirling flow with a vortex breakdown using modified shear stress transport model," *Industrial & Engineering Chemistry Research*, vol. 60, no. 16, pp. 6016–6026, 2021.

[2] Y. H. Alahmadi and A. F. Nowakowski, "Modified shear stress transport model with curvature correction for the prediction of swirling flow in a cyclone separator," *Chemical Engineering Science*, vol. 147, pp. 150–165, 2016.

[3] M. R. Birajdar and S. A. Kale, "Performance analysis of new airfoils and blade for a small wind turbine," *International Journal of Energy, Environment and Economics*, vol. 24, no. 1, pp. 75–86, 2016.

[4] L. F. Chen, J. Zang, A. J. Hillis, G. C. J. Morgan, and A. R. Plummer, "Numerical investigation of wave–structure interaction using OpenFOAM," *Ocean Engineering*, vol. 88, pp. 91–109, 2014.

[5] A. Crasta, S. Pavitra, and S. A. Khan, "Estimation of surface pressure distribution on a delta wing with curved leading edges in hypersonic/supersonic flow," *International Journal of Energy, Environment and Economics*, vol. 24, no. 1, pp. 67–73, 2016.

[6] A. M. Gooray, C. B. Watkins, and W. Aung, "Improvements to the k-epsilon model for calculations of turbulent recirculating flow," in *4th Symposium on Turbulent Shear Flows*, 1984, pp. 18–26.

[7] C. J. Greenshields, *OpenFOAM User Guide. Version 2.4.0*, OpenFOAM Foundation Ltd, 2015.

[8] R. Guo, Y. Bai, X. Pei, and Z. Lai, "Numerical investigation of aerodynamics and wake on biplane airfoils at high angles of attack," *International Journal of Mechanical Sciences*, vol. 205, pp. 106606, 2021.

[9] A. Hellsten, "Some improvements in Menter's k-ω SST turbulence model," in *AIAA 2554*, 1998.

[10] J. H. G. Howard, "Flow prediction in rotating ducts using Coriolis-modified turbulence models," *Journal of Fluids Engineering*, vol. 102, pp. 456–461, 1980.

[11] A. Khodak and C. Hirsch, "Second-order nonlinear k-ε models with explicit effect of curvature and rotation," in *ECCOMAS Computational Fluid Dynamics Conference*, 1996, pp. 690–696.

[12] D. Knight and P. Saffman, "Turbulence model predictions for flows with significant mean streamline curvature," in *16th Aerospace Sciences Meeting*, 1978, pp. 258.

[13] C. L. Ladson, "Effects of independent variation of Mach and Reynolds numbers on the low-speed aerodynamic characteristics of the NACA 0012 airfoil section," *NASA Technical Paper 4074*, National Aeronautics and Space Administration, Scientific and Technical Information Division, 1988.

[14] S. W. Park and M. K. Chung, "Curvature-dependent two-equation model for prediction of turbulent recirculating flows," *AIAA Journal*, vol. 27, no. 3, pp. 340–344, 1989.

[15] P. E. Smirnov and F. R. Menter, "Sensitization of the SST turbulence model to rotation and curvature by applying the Spalart–Shur correction term," *Journal of Turbomachinery*, vol. 131, no. 4, pp. 1–8, 2009.

[16] P. R. Spalart and M. Shur, "On the sensitization of turbulence models to rotation and curvature," *Aerospace Science and Technology*, vol. 1, no. 5, pp. 297–302, 1997.

[17] Q. Zhang and Y. Yang, "A new simpler rotation/curvature correction method for Spalart–Allmaras turbulence model," *Chinese Journal of Aeronautics*, vol. 26, no. 2, pp. 326–333, 2013.